In-vivo Proton MR Spectroscopic Imaging of Glycine in Brain Tumors at 3.0 T

S. K. Ganji[1], I. E. Dimitrov[1,2], E. A. Maher[3], and C. Choi[1]
[1]Advanced Imaging Research Center, University of Texas Southwestern Medical Center, Dallas, Texas, United States, [2]Philips Medical Systems, Cleveland, Ohio, United States, [3]Internal Medicine and Neurology, University of Texas Southwestern Medical Center, Dallas, Texas, United States

INTRODUCTION

Recent studies have shown that abnormal glycine (Gly) levels are implicated in several brain disorders, in particular, malignant tumors [1-3]. Most of in-vivo Gly detection relied on single-voxel spectroscopy, which does not provide regional distribution of the metabolite. We report spectroscopic imaging (SI) of Gly in brain tumors using a PRESS based method with an optimized echo time (TE) [4]. Preliminary in vivo data from brain tumor patients are presented.

METHODS

PRESS TE = 160 (TE1 = 60, TE2 = 100) ms was used for SI of Gly, at which the Gly singlet at 3.55 ppm can be differentiated from the myo-inositol (mIns) multiplet. Experiments were carried out on a 3.0 T whole-body scanner (Philips Medical Systems) with a body coil for transmission and an 8-channel phased array head coil for reception. The sequence was tested in a spherical phantom (6 cm diameter) with Gly (2mM), mIns (8mM), N-acetyl-aspartate (NAA) (20mM), creatine (Cr) (16 mM), glutamate (Glu) (20mM), and glutamine (Gln) (6mM). In vivo data were obtained from 10 patients with gliomas. Written informed consent was obtained prior to the scans. Following survey scans, T_2w FLAIR images (axial and sagittal) were acquired to identify tumor regions. Chemical shift imaging (CSI) data were acquired using a PRESS-based 2D SI sequence with field of view (FOV) of 20x16 cm^2, spatial resolution of 1x1 cm^2, and slice thickness of 1.5 cm. Acquisition parameters included: TR = 1.2 s; 1024 complex sampling points; spectral width of 2000 Hz; number of averages = 2. Outer-volume suppression bands were positioned to minimize the signals from subcutaneous region. Water suppression was achieved using four RF-pulses. Single-voxel localized data were additionally obtained from a 2x2x2 cm^3 voxel positioned within the enhanced-FLAIR region (TR = 2 s; 128 averages). In the data analysis, residual water signal was removed using the HL-SVD filter of the JMRUI [5] and frequency-drift corrections were performed using in-house Matlab programs. Subsequently, LCModel software [6] was used for analyzing the CSI multi-pixel data, using basis sets created with published chemical shift and coupling constants [7].

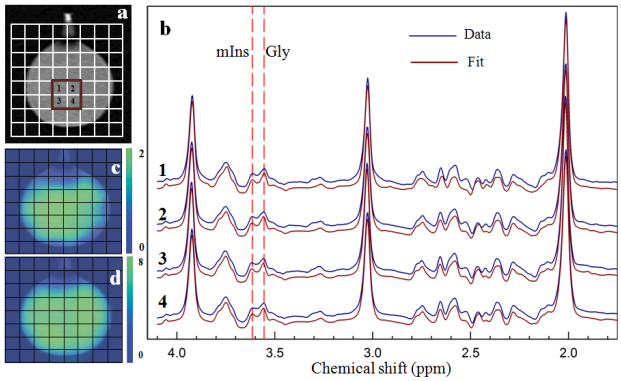

Fig. **1**: (**a**) CSI grid position in the phantom. (**b**) LCModel results for the four selected voxels (shown as brown bax in Fig. 1a) along with LCModel fits. Vertical lines indicate Gly and mIns signals. (**c**) and (**d**) shows the Gly and mIns concentration maps respectively (in mM).

RESULTS AND DISCUSSION

Fig. 1 displays SI spectra and metabolite concentration maps from the phantom. The spectral pattern obtained from the phantom was consistent with the reported simulated spectrum at TE = 160 ms [4]. Figure 2 shows the axial images and spectra from a glioblastoma (GBM) patient. The spectra within the enhanced-FLAIR region show elevated Gly and Cho. Increases of these metabolites were clearly indicated in the concentrations maps in Figs. 2b and 2c. Figure 3 shows the comparison between SI and single-voxel localized MRS data from the tumor mass region. The spectral pattern and signal intensity ratios agreed well between CSI and single-voxel data. The Gly concentrations were all estimated to be ~5 mM in Figs. 2a (spectra 1 and 2) and 2b, with CRLBs less than 5%. Figure 4 shows a Gly map obtained from another GBM patient. In addition, five patients showed elevated Gly within the enhanced-FLAIR regions, concentrations being 3-6 mM, with CRLBs less than 15%. In conclusion, the optimized-TE PRESS-based SI method can be used for obtaining the regional distribution of Gly levels. Elevation of Gly may be used as a biomarker of malignant gliomas and thus measurement of its spatial distribution may improve our understanding of tumor proliferation.

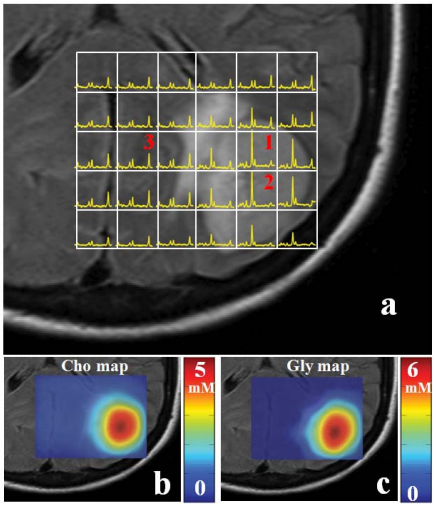

Fig. **2**: (**a**) CSI grid display and spectra in a GBM patient. Spectra of labeled voxels in (a) are shown in Fig. 3a. (**b**) and (**c**) show Cho and Gly concentration maps from LCModel analyses of individual spectra, respectively.

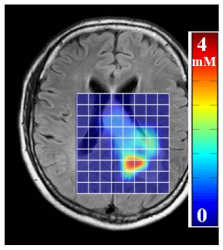

Fig. **4**: Gly concentration map from a GBM patient.

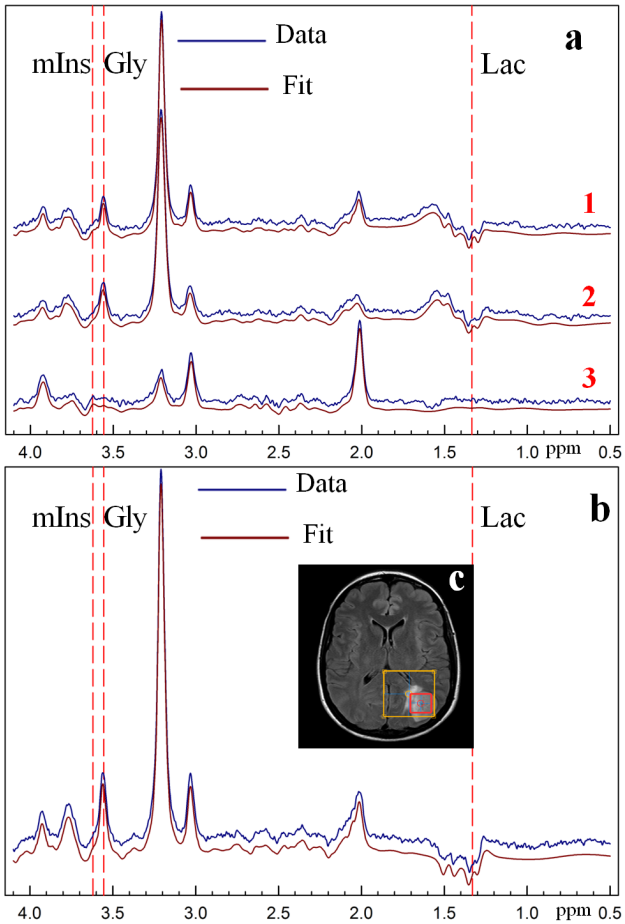

Fig. **3**: (**a**) Spectra for the pixels indicated in Fig. **2a** together with LCModel fits. (**b**) A single-voxel-localized spectrum (PRESS TE = 160ms) obtained from a voxel shown in an image. Vertical lines indicate Gly, mIns and Lac peak locations.

REFERENCES

1. Hattingen E *et al*. MAGMA 2009;22:33-41. **2**. Bruhn H *et al*. NMR Biomed 1992;5:253-258. **3**. Davies NP *et al*. NMR Biomed 2010;23:80-87. **4**. Choi C *et al*. ISMRM 2010. Stockholm. p. 3329. **5**. Naressi A. *et al*. MAGMA 2001;12:141–152. **6**. Provencher SW Magn Reson Med 1993;30:672-679. **7**. Govindaraju V *et al*. NMR Biomed 2000;13:129-153.